Automatic Correction of Motion Artifacts in 4D Left Ventricle Model Reconstructed from MRI

Yi Su[1], May-Ling Tan[1], Chi-Wan Lim[1], Soo-Kng Teo[1], Senthil Kumar Selvaraj[1], Min Wan[1], Liang Zhong[2,3], Ru-San Tan[2,3]

[1]Institute of High Performance Computing, A*STAR, Singapore
[2]National Heart Centre, Singapore
[3]Duke-NUS Graduate Medical School, Singapore

Abstract

This paper describes a computer method to correct the shape of three-dimensional (3D) left ventricle (LV) models created from magnetic resonance imaging (MRI) data that is affected by patient motion during scanning. Three-dimensional meshes of the LV endocardial and epicardial surfaces are created from border-delineated MRI data at every time frame of the cardiac cycle to generate a time-series model of the heart. A geometrically-based approach is used to achieve smooth epicardial shapes by iterative in-plane translation of vertices in the LV model. The Principal Curvatures of the LV epicardial surfaces across multiple time frames are used to construct a shape-based optimization objective function to restore the shape of the LV via a dual-resolution semi-rigid deformation process and a free-form geometric deformation process. A limited memory quasi-Newton algorithm, L-BFGS-B, is then used to solve the optimization problem. We tested our algorithm on 9 patient-specific models and it was able to correct motion artifacts without altering the general shape of the heart, such as its asymmetrical shape. The magnitudes of in-plane translations (Δx = 0.972±0.857 mm and Δy =1.306±1.290 mm in the x- and y-directions, respectively) are also within the range of published experimental findings. The average computational time to correct each 4D model is 6 min 34 s.

1. Introduction

Breath-hold cine Magnetic Resonance Imaging (MRI) is an established imaging technique for assessment of cardiac morphology and function in clinical practice. However, factors such as respiration and patient movement contribute to misalignments in the MRI data which results in inaccuracies. Image registration techniques are often used to correct these misalignments. In [1], a number of cardiac image registration methods were reviewed and these are categorized into geometric image feature approach and voxel similarity measure approach. Other methods include the external skin marker-based techniques [2], landmark-based techniques [3] and thorax surface-based techniques [4]. More recently, the method proposed in [5] demonstrated the use of constrained optimization of the intensity similarity of intersecting image lines.

In this work, we deviate from the typical image-based approach to develop an automatic shape-driven algorithm to restore the shape of a 4D (i.e., spatial + time) left ventricular (LV) models reconstructed from MRI data. The basic premise is that the LV epicardial surface must be smooth after the restoration process and that the general shape of the LV cannot be lost in the process. The *Principal Curvatures* (κ_1 and κ_2) are used as geometric measures to quantitate the smoothness of the LV endocardial surfaces.

2. Method

Three-dimensional meshes of the LV endocardial and epicardial surfaces are created from border-delineated MRI data at every time frame of the cardiac cycle to generate a time-series model of the heart. A geometrically-based approach is used to achieve smooth epicardial shapes by iterative in-plane translation of vertices in the LV model. The Maximum Principal Curvature (κ_1) and the Minimum Principal Curvature (κ_2) of the LV epicardial surfaces across multiple time frames are used to construct a shape-based optimization objective function to restore the shape of a motion-affected LV via a dual-resolution semi-rigid deformation process and a free-form geometric deformation process. A limited memory quasi-Newton algorithm, L-BFGS-B, is then used to solve the optimization problem.

2.1. Overview

As the 4D LV model is reconstructed from contours of the myocardial borders, the restoration process works by progressive translation of these contours in the plane of their respective short-axis (SA) slice. Figure 1 illustrates the shifting of the contour on a SA slice in the in-plane direction. This can be considered as a semi-rigid modification since the shape of the contour within each plane is kept constant during the translation.

The shape restoration is performed towards the goal that the LV epicardial surface must be smooth. This implies that the surface has minimum concavity. Hence, a suitable objective function F takes the form of

$$F = \sum_{j=1}^{n}\sum_{i=1}^{m}\left\{\| \kappa_{1,i} \| \mid \kappa_{1,i} < 0 + \| \kappa_{2,i} \| \mid \kappa_{2,i} < 0\right\}_j \qquad (1)$$

where $\kappa_{1,i}$ and $\kappa_{2,i}$ are the maximum and minimum principal curvature computed at vertex i, respectively; and m is the total number of vertices in the epicardial surface mesh of frame j such that n is the total number of frames in the whole cardiac cycle.

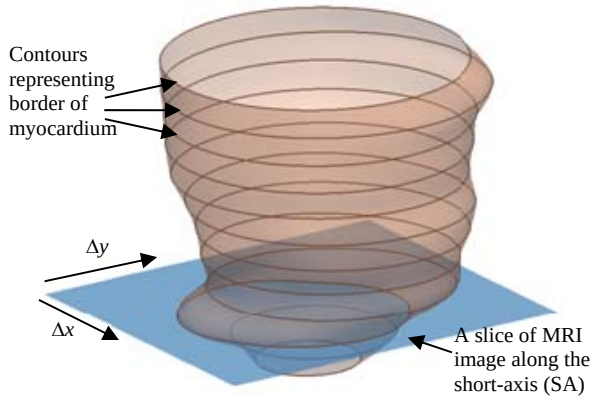

Figure 1. Modifying shape of LV epicardial surface mesh by translating the contours on SA slice.

2.2. Calculation of principal curvatures

To compute the principal curvatures of the LV epicardial surface mesh, a quadric fitting method is used to approximate the underlying geometry at every vertex of the LV endocardial mesh. A quadric surface S in 3D space can be expressed in the parametric form

$$S(u,v) = \begin{bmatrix} u & v & au^2 + buv + cv^2 + du + ev \end{bmatrix}^T \qquad (2)$$

where u and v are the surface parameters and $\{a, b, c, d, e\}$ are the quadric coefficients. To define S at a vertex p, we select the neighboring points in the vicinity of p, which is called the n-ring. The quadric coefficients can then be determined by solving a system of linear equations associated with the n-ring neighborhood using a least square method [6].

The first fundamental matrix (G) and second fundamental matrix (D) of S are given by

$$G = \begin{bmatrix} S_u \cdot S_u & S_u \cdot S_v \\ S_u \cdot S_v & S_v \cdot S_v \end{bmatrix} = \begin{bmatrix} E & F \\ F & G \end{bmatrix} \qquad (3)$$

$$D = \begin{bmatrix} S_{uu} \cdot \hat{n} & S_{uv} \cdot \hat{n} \\ S_{uv} \cdot \hat{n} & S_{vv} \cdot \hat{n} \end{bmatrix} = \begin{bmatrix} L & M \\ M & N \end{bmatrix} \qquad (4)$$

and the unit surface normal is given by $\hat{n} = (S_u \times S_v)/|S_u \times S_v|$. The principal curvatures are expressed as

$$\kappa_1 = \frac{B + \sqrt{B^2 - A^2(4ac - b^2)}}{A^3} \qquad (5)$$

$$\kappa_2 = \frac{B - \sqrt{B^2 - A^2(4ac - b^2)}}{A^3} \qquad (6)$$

where $A = \sqrt{d^2 + e^2 + 1}$ and $B = a + ae^2 + c + cd^2 - bde$.

The value of n-ring used in the quadric fitting affects is an important consideration since it determines how sensitive the fitting process is to the effect of geometrical variation. With a bigger n-ring value, the fitting is less sensitive to high frequency variations. With a smaller n-ring value, localized variation in shape is captured.

2.3. Optimization

We minimize the non-linear objective function in Eqn. (1) using the L-BFGS-B algorithm [7], which is adept at solving multivariate nonlinear bound-constrained optimization problems. It is based on the gradient projection method and utilizes a limited-memory BFGS matrix to approximate the Hessian of the objective function. The optimization algorithm does not store the results from all iterations but only a user-specified subset. The advantage is that the simple approximations of the Hessian matrices allows fast linear convergence and requires minimal storage [7] while giving good results.

To set up the optimization problem, we write Eqn. (1) as $F(\mathbf{x})$ with n variables, such that $\mathbf{x}$ contains the centroid coordinates (X_C, Y_C) of the contours on the SA slices, i.e.,

$$\mathbf{x} = \begin{Bmatrix} x_1 = X_{C,1} \\ x_2 = Y_{C,1} \\ x_3 = X_{C,2} \\ x_4 = Y_{C,2} \\ \vdots \quad \vdots \quad \vdots \\ x_{n-1} = X_{C,N} \\ x_n = Y_{C,N} \end{Bmatrix}$$

Each of the variables x_i in $F(\mathbf{x})$ is subjected to the bounded-constraints

$$lb_i \le x_i \le ub_i \qquad i = 1, 2, 3, \ldots, n \tag{7}$$

where lb_i and ub_i are the lower and upper bounds of x_i, respectively. In this work, the variables are constrained to translate within a bound of ±20 mm. This value is consistent with what was observed experimentally [8] (expected to be in the range of 0 to 21 mm).

In addition, the gradient g_i associated with each variable x_i must also be defined such that $g_i = \partial F(x) / \partial x_i$. Since $F(\mathbf{x})$ is in a non-analytical form, we approximate g_i using the forward difference method, i.e.,

$$g_i = \frac{F(x_1, \cdots, x_i + \Delta x_i, \cdots, x_n) - F(x_1, \cdots, x_i, \cdots, x_n)}{\Delta x_i} \tag{8}$$

where Δx_i is a small increment in x_i.

2.4. Dual-resolution deformation

To retain the general variation of the LV shape, we perform the optimization in two phases. In the first phase, optimization was performed using an *n*-ring of 5 for the surface fitting process. This restores the mesh with respect to low frequency geometrical variation to produce the intermediate mesh. In the second phase, optimization was performed using an *n*-ring of 2. This further minimizes the surface concavity of the intermediate mesh over a localized region. The results from setting *n*-ring value = 5 and then *n*-ring = 2 are shown in Figure 22. As observed, the end result restores smoothness with minimum principal curvature to the LV heart.

Figure 2. Dual-resolution deformation: (a) original mesh with motion artifact, (b) intermediate mesh after optimization using *n*-ring = 5, and (c) final mesh after optimization using *n*-ring = 2.

3. Results

Nine patient-specific 4D LV models reconstructed from MRI data containing motion artifacts. The MRI scan was performed using breath-held steady-state free precession technique on a 1.5T Siemens scanner (Avanto, Siemens Medical Solutions, Erlangen). TrueFISP (fast imaging with steady-state precession) MR pulse sequence with segmented k-space and retrospective electrocardiographic gating were used to acquire 2D cine images of the LV in the LA plane, as well as a parallel stack of 2D cine images of the LV in the SA plane, from the LV base to apex (8 mm interslice thickness, no interslice gap). Each slice was acquired in a single breath hold, with 22 temporal phases per heart cycle.

The epicardial and endocardial borders of contiguous SA slices were manually delineated by an experienced cardiologist using a commercially-available software CMRtools (Cardiovascular Imaging Solution, UK). Mesh models were reconstructed from these contours and used as input to our algorithm.

From the results, the magnitudes of in-plane translations are Δx = 0.972±0.857 mm and Δy = 1.306±1.290 mm in the *x*- and *y*-directions, respectively. These values are within the range of published findings [1]. The qualitative result of one particular sample is shown in Fig. 3. The figure illustrates that our method is able to correct motion artifacts without altering the general shape of the heart, such as its asymmetrical shape. The average computational time to correct each 4D model is approximately 6 min 34 s.

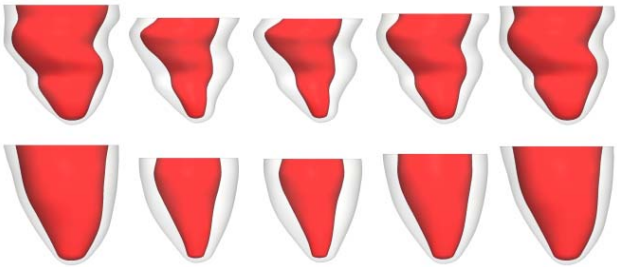

Figure 3. Shape restoration of 4D model over whole cardiac cycle; top row: original model; bottom row: restored model.

4. Discussion

From the results, we observed that the shape restoration of the LV epicardial surface was successful. Visually, we verified that the asymmetry of the LV geometry was preserved while the geometrical irregularities on the LV epicardial surface were significantly reduced. Quantitatively, the magnitude of negative κ_1 and κ_2 values were reduced considerably after the shape restoration, as shown in Fig. 4. This indicates that regions with concavity is reduced.

Validation of our shape restoration technique with clinical results is important for the method to be accepted clinically. Registration methods are often validated using external markers or anatomical landmarks [9]. However, such validations are difficult because they are not readily available. In our work, we compared the mean contour displacement values of our method with those of existing image registration techniques [1], where the minimum

and maximum translations in the *x*- and *y*-directions lie between 0 to 4.8 mm. In comparison, our results lie in the range of 0.1 to 2.6 mm. Also, we observed that the translation in the *y*-direction is more than in the *x*-direction. This indicates that motion artifact occurs more prominently in the anterior-inferior direction (*y*-direction) as compared to the septal-lateral direction (*x*-direction), which suggests that breathing during image acquisition could be the likely cause of motion artifact.

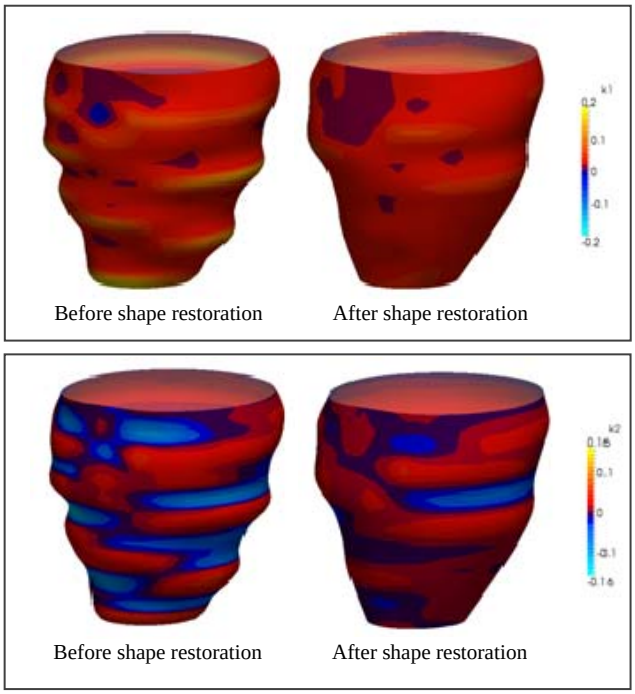

Figure 4. Change in curvature values of epicardial surface before and after restoration: (a) maximum principal curvature κ_1, (b) minimum principal curvature κ_2

5. Conclusion

The proposed solution is a viable software-based alternative to correct MRI data affected by patient motion without the need of addition hardware-based motion registration tools. It is sufficiently efficient for real clinical utilization.

Acknowledgements

This work was supported by the Science and Engineering Research Council (SERC), Agency for Science, Technology and Research (A*STAR) Singapore through the award of Project Grant 132 148 0012.

References

[1] Mäkelä T, Clarysse P, Sipilä O, Pauna N, Pham QC, Katila T, Magnin IE. A review of cardiac image registration methods. IEEE Transaction on Medical Imaging 2002;21:1011-21.

[2] Li Q, Zamorano L, Jiang Z, Vinas F, Diaz F. The application accuracy of the frameless implantable marker system and analysis of related affecting factors. Lecture Notes in Computer Science 1496: Medical Image Computing and Computer-Assisted Intervention, MICCAI98, WM Wells, A Colchester, and S Delp, Eds., 1998:253-60.

[3] Eberl S, Kanno I, Fulton RR, Ryan A, Hutton BF, Fulham MJ. Automated interstudy image registration technique for SPECT and PET. J. Nucl. Med. 1996;37:137-45.

[4] Klein GJ, Huesman RH. Four-dimensional processing of de- formable cardiac PET data. Med Image Anal 2002;6:29-46.

[5] Elen A, Hermans J, Ganame J, Loeckx D, Bogaert J, Maes F, Suetens P. Automatic 3-D breath-hold related motion correction of dynamic multislice MRI. IEEE Transaction on Medical Imaging 2010;29:868-78.

[6] Su Y, Zhong L, Lim CW, Ghista D, Chua T, Tan RS. A geometrical approach for evaluating left ventricular remodeling in myocardial infarct patients. Comput. Methods Programs Biomed 2012;108:500-10.

[7] Zhu CY, Byrd RH, Lu PH, Nocedal J. L-BFGS-B: Fortran Subroutines for large-scale bound constrained optimization. ACM Transactions on Mathematical Software (TOMS) 1997;23:550-60.

[8] McLeish K, Hill DLG, Atkinson D, Blackall JM, Razavi R. A study of the motion and deformation of the heart due to respiration. IEEE Transaction on Medical Imaging 2002;21:1142-50.

[9] Woods RP. Validation of registration accuracy. In: Isaac Bankman, editor. Handbook of Medical Imaging: Processing and Analysis. New York: Academic, 2000:569-76.

Address for correspondence.

Yi Su
1 Fusionopolis Way, #16-16 Connexis, Singapore 138632, Republic of Singapore
suyi@ihpc.a-star.edu.sg